MicroRNA-433 inhibits cell growth and induces apoptosis in human cervical cancer through PI3K/AKT signaling by targeting FAK

JIE XU[1,2], WEIPEI ZHU[1], LIJUAN CHEN[1] and LILI LIU[1]

[1]Department of Obstetrics and Gynecology, The Second Affiliated Hospital of Suzhou University, Suzhou, Jiangsu 215000; [2]Department of Obstetrics and Gynecology, Zhangjiagang First People's Hospital, Zhangjiagang, Jiangsu 215600, P.R. China

Received January 6, 2018; Accepted August 17, 2018

DOI: 10.3892/or.2018.6718

Abstract. The present study aimed to examine the role of microRNA-433 in the growth and death of cervical cancer cells. RNA isolation, reverse transcription-quantitative polymerase chain reaction analysis, an MTT assay, flow cytometry, and western blot analysis were used for this investigation. The results showed that the expression of microRNA-433 was downregulated in patients with cervical cancer. The disease-free survival and overall survival rates of patients with low expression levels of microRNA-433 were lower, compared with those in patients with high expression levels of microRNA-433. The expression levels of microRNA-433 were downregulated in cervical cancer *in vitro*. It was found that the downregulation of microRNA-433 promoted the growth and inhibited the apoptosis of cervical cancer cells through activating focal adhesion kinase (FAK)/phosphoinositide 3-kinase (PI3K)/AKT signaling. However, the upregulation of microRNA-433 induced apoptosis and suppressed the growth of cervical cancer cells through inhibiting the FAK/PI3K/AKT signaling pathway. In addition, FAK or PI3K inhibitors promoted the death of cervical cancer cells following the downregulation of microRNA-433. These results revealed that microRNA-433 suppressed the growth of cervical cancer cells via the FAK/PI3K/AKT signaling pathway.

Introduction

Cervical cancer is the most common malignancy and one of the causes of cancer-associated mortality. It has also been verified that high risk human papilloma virus (HR-HPV) infection is essential for cervical cancer (1). Harald Chuer Hausen made significant contributions to the current understanding of HPV and was thus awarded the 2008 Nobel Prize in Physiology or Medicine. Evidence has indicated that the progression of HPV infection into cervical cancer is a progressive and slow process. There is a definite precancerous lesion stage, which is cervical intraepithelial neoplasia. This has provided favorable timing in terms of inhibition (2). However, treatment targeting cervical cancer is dominated by destructive surgery at present (2), with non-invasive and effective drug inhibiting methods lacking (3).

RNomics is the study of all RNA structures and functions at the genomic level, including non-coding RNA and mRNA (4). The Human Genome Project, completed in 2001, (4) marked the beginning of the post-genome era (5). It has led to our current interpretation of the composition and expression regulation of genetic information from non-coding RNA (5). Non-coding RNA, particularly microRNAs (miRNAs), is important in regulating gene expression (6).

Focal adhesion kinase (FAK) is a key non-receptor tyrosine protein kinase in signal transduction (7). It is closely associated with all vital cellular activities (7). In addition, it is involved in tumor invasion and metastasis. Evidence indicates that the expression of FAK is upregulated in invasive cells, including those in ovarian and endometrial cancer, and thyroid carcinoma (6). Activated FAK can activate multiple signal transduction pathways through multiple downstream signal transduction-associated molecules (6,8). Therefore, it is involved in cell proliferation, differentiation, extension, migration, tumor invasion, and metastasis (7).

The Akt/mammalian target of rapamycin (mTOR) signaling pathway is involved in regulating multiple cellular behaviors, including cell proliferation, survival, growth, and migration (9). The association of such a signaling pathway with tumor genesis has been investigated extensively (10). It is been found that the transformation or deletion of certain molecules in the phosphoinositide 3-kinase (PI3K)/Akt/mTOR signaling pathway is closely associated with tumor genesis (11). These tumors include breast, ovarian and endometrial cancer, and melanoma. The present study aimed to examine the role of microRNA-433 in cell growth and death in cervical cancer.

Correspondence to: Dr Weipei Zhu, Department of Obstetrics and Gynecology, The Second Affiliated Hospital of Suzhou University, 1055 Sangxiang Road, Suzhou, Jiangsu 215000, P.R. China
E-mail: weiliaochuang@163.com

Key words: microRNA-433, cervical cancer, focal adhesion kinase, phosphoinositide 3-kinase, AKT

Materials and methods

Patients and clinical data collection. Patients with cervical cancer (n=72, 57±7 years age, female) and healthy volunteers (n=12, 52±5 years age, female) were recruited from the Department of Obstetrics and Gynecology, The Second Affiliated Hospital of Suzhou University (Suzhou, China). Peripheral blood samples from the patients and volunteers (10 ml) were centrifuged at 1,000 x g for 5 min at 4˚C and serum was stored at -80˚C. The patients with cervical cancer were examined every three months for 5 years.

RNA isolation and reverse transcription-quantitative polymerase chain reaction (RT-qPCR) analysis. Total RNA from the clinical samples and cultured cells was extracted using TRIzol (Invitrogen; Thermo Fisher Scientific, Inc., Waltham, MA, USA). cDNA was were obtained using M-MLV reverse transcriptase (Promega Corporation, Madison, WI, USA) at 37˚C for 30 min, and 84˚C for 10 sec. RT-qPCR analyses were performed using Platinum SYBR-Green qPCR SuperMix-UDG reagents (Invitrogen; Thermo Fisher Scientific, Inc.). miRNA-26b: Forward, 5'-GGATCATGA TGGGCTCCT-3' and reverse, 5'-CAGTGCGTGTCGTGG AGT-3'; U6: Reverse, 5'-GGAACGCTTCACGAATTTG-3' and forward, 5'-ATGTTCTGGTGTCCTCAAATG-3'. The conditions were 10 min at 95˚C, 40 cycles of 95˚C for 15 sec, 60˚C for 30 sec and 72˚C for 30 sec. Expression levels of miRNA-26b were calculated using the $2^{-\Delta\Delta Cq}$ method (12).

GeneChip array. Total RNA was hybridized using SurePrint G3xWhole Genome GE 8x60 K Microarray G4852A platform (Stratagene). Results were quantified using Agilent Feature Extraction Software (version A.10.7.3.1).

Cell culture and cell transfection. The CaSki human cervical cancer cell line was purchased from the American Type Culture Collection (Manassas, VA, USA) and cultured in Dulbecco's modified Eagle's medium (DMEM; Sigma; EMD Millipore, Billerica, MA, USA) supplemented with 10% fetal bovine serum (FBS; Gibco; Thermo Fisher Scientific, Inc.) at 37˚C and 5% CO_2. FAK plasmid (5'-ACCATGAACACCGCGGGAGC-3' and 5'-ACG GCCACGCGTAATTCTAA-3') was purchased from Sangon Biotech Co., Ltd. (Shanghai, China). The microRNA-433 (5'-UGG AAGACUAGUGAUUUUGUUGU-3'), anti-microRNA-433 (5'-UCAACAUCAGUCUGAUAAGCUA-3') and negative mimics (5'-UUGUACUACACAAAAGUACUG-3') were transfected using Lipofectamine 2000 (Invitrogen; Thermo Fisher Scientific, Inc.), according to the manufacturer's protocol. After transfection for 4 h, 0.1 nM of GDC-0032 (MedChemExpress), an Akt inhibitor was added into cell for 44 h.

Proliferation assay. The cells (10^3 cell/well) were cultured in 96-well plates and MTT solution was added to the cells at 37˚C and 5% CO_2 for 4 h. The medium was removed and DMSO was added to the cells for 20 min at 37˚C. Cell proliferation was determined using a microplate reader (Bio-Rad Laboratories, Inc., Hercules, CA, USA) at 492 nm.

Analysis of metastatic rate. The cells ($2x10^5$ cells/ml) were cultured in 24-well plates and seeded in the upper chamber of Costar Transwell culture plates (8 μm). DMEM with 20% FBS was added to the lower chamber for 24 h at 37˚C and 5% CO_2. The chamber was washed with PBS and the cells were fixed in 4% paraformaldehyde for 15 min. The cells were stained with crystal violet and the number of migrated cells was counted under a Nikon Eclipse 80i microscope (Nikon Corporation, Tokyo, Japan).

Flow cytometry. The cells were cultured in 6-well plates and washed with PBS. FITC Annexin V (5 μl) and propidium iodide (PI) (5 μl) were added to the cells and stained for 15 min in the dark. Apoptosis was examined on a FACSCalibur flow cytometer (BD Biosciences, San Jose, CA, USA) immediately following this.

Western blot analysis. The cell proteins of each sample were extracted using RIPA buffer (Beyotime Institute of Biotechnology, Haimen, China). The total protein (50 μg) in each sample was loaded and electrophoresed by 6-15% SDS-PAGE and then transferred onto polyvinylidene fluoride membranes. The membranes was blocked with 5% w/v skimmed milk powder for 1 h at room temperature, and incubated with antibodies against FAK (cat. no. sc-24545, 1:500; Santa Cruz Biotechnology, Inc., Dallas, TX, USA), phosphorylated (p)-AKT (cat. no. sc-7985-R, 1:500; Santa Cruz Biotechnology, Inc.), B-cell lymphoma 2 (Bcl-2)-associated X protein (Bax; cat. no. sc-4239, 1:1,000; Santa Cruz Biotechnology, Inc.), p53 (sc-47698, 1:1,000; Santa Cruz Biotechnology, Inc.), MDM2 (sc-812, 1:1,000; Santa Cruz Biotechnology, Inc.) and GAPDH (cat. no. sc-293335, 1:5,000; Santa Cruz Biotechnology, Inc.) at 4˚C. The membranes were washed with TBST and incubated with horseradish peroxidase-conjugated goat anti-rabbit secondary antibody (1:5,000, cat. no. 7074; Cell Signaling Technology, Inc., Danvers, MA, USA) for 1 h at room temperature. The protein bands were visualized by enhanced chemiluminescence (P0018A, BeyoECL Star; Beyotime Institute of Biotechnology) and observed using ImageQuant LAS 4000 mini (General Electric Company, Boston, MA, USA).

Caspase-3 and caspase-9 activity levels. The cell proteins of each sample were extracted using RIPA buffer (Beyotime Institute of Biotechnology). The total protein (10 μg) was used to analyze the activities of caspase-3 and caspase-9 using caspase-3 and caspase-9 activity kits (Beyotime Institute of Biotechnology). The activities of caspase-3 and caspase-9 were determined using a microplate reader (Bio-Rad Laboratories, Inc.) at 405 nm.

Immunofluorescence staining. The cells were washed with PBS and fixed with 4% paraformaldehyde for 15 min. The cells were permeabilized with 0.2% Triton X-100 in PBS for 15 min at room temperature, followed by blocking with 5% BSA (Beyotime Institute of Biotechnology) in PBS for 1 h at room temperature. Cell immunostaining was then performed via incubation with FAK antibody (1:100) at 4˚C overnight. The cells were washed with PBS and incubated with 555-secondary goat anti-rabbit antibodies (sc-362272, 1:100; Santa Cruz Biotechnology, Inc.) for 1 h at room temperature. The cells were stained with DAPI for 30 min in the dark at

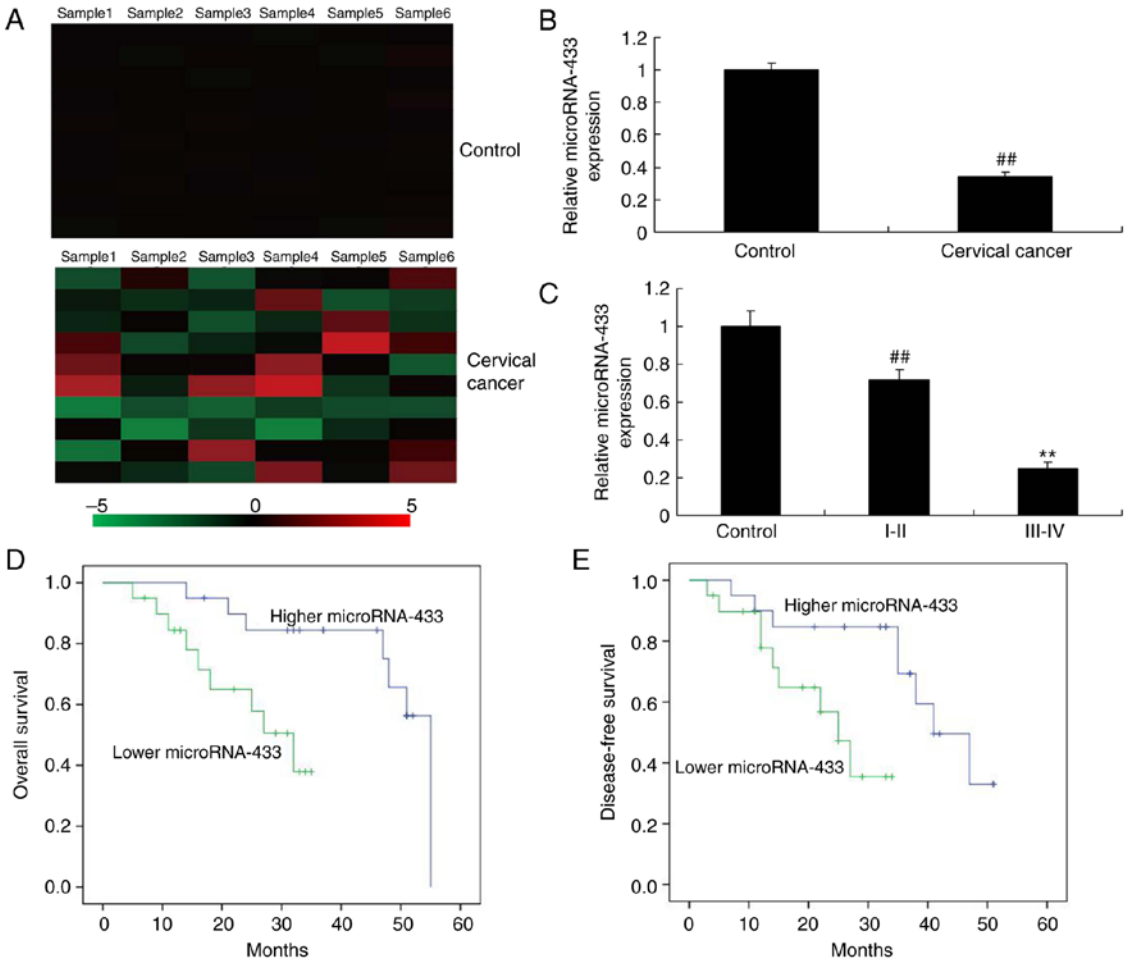

Figure 1. Expression levels of microRNA-433 in patients with cervical cancer. (A) GeneChip and (B) reverse transcription-quantitative polymerase chain reaction analyses for the expression levels of microRNA-433 in patients with cervical cancer. (C) Expression levels of microRNA-433 in patients with cervical cancer of different clinical stages (I-II and III-IV). Correlation of the expression of microRNA-433 with (D) OS and (E) DFS rate. Data are presented as the mean ± standard deviation. $^{\#\#}$P<0.01, vs. control; **P<0.01, vs. I-II group. Control, healthy volunteers; OS, overall survival; DFS, disease-free survival.

room temperature. Immunofluorescent images were captured and viewed with a Nikon Eclipse 80i microscope.

Statistical analysis. Data are presented as the mean ± standard deviation. Significant differences between groups were compared using Student's t-test or one-way analysis of variance and Tukey's post hoc test. P<0.05 was considered to indicate a statistically significant difference.

Results

Expression levels of microRNA-433 in patients with cervical cancer. Initially, the expression of microRNA-433 was analyzed using a GeneChip array, which suggested that microRNA-433 was downregulated in patients with cervical cancer, compared with the control group (Fig. 1A). Subsequently, the expression of microRNA-433 was analyzed using RT-qPCR analysis, which suggested that the expression of microRNA-433 was downregulated in the patients with cervical cancer, compared with the control group (Fig. 1B). In addition, the expression levels of microRNA-433 in patients with cervical cancer at stage III-IV were lower than those of patients with cervical cancer at stage I-II (Fig. 1C). Subsequently, the associations between the expression of microRNA-433 expression and disease-free survival (DFS) and overall survival (OS) rates were examined. As shown in Fig. 1D and E, the DFS and OS rates in patients with low expression levels of microRNA-433 were lower, compared with those in patients with high expression levels of microRNA-433. These results indicated that microRNA-433 has a significant role in cervical cancer.

Downregulation of microRNA-433 promotes the growth and inhibits the apoptosis of cervical cancer cells. The role of microRNA-433 in the growth of cervical cancer cells was examined, which suggested that the expression of microRNA-433 was downregulated following transfection with anti-microRNA-433 mimics, compared with that in the negative control group (Fig. 2A). The downregulation of microRNA-433 promoted growth and metastasis, and inhibited the apoptosis and caspase-3/-9 activity of cervical cancer cells, compared with the control group (Fig. 2B-H). These results indicated that the downregulation of microRNA-433 promoted the growth and inhibited the apoptosis of cervical cancer cells.

Upregulation of microRNA-433 reduces the growth and promotes the apoptosis of cervical cancer cells. The expression of microRNA-433 was upregulated in cervical cancer cells

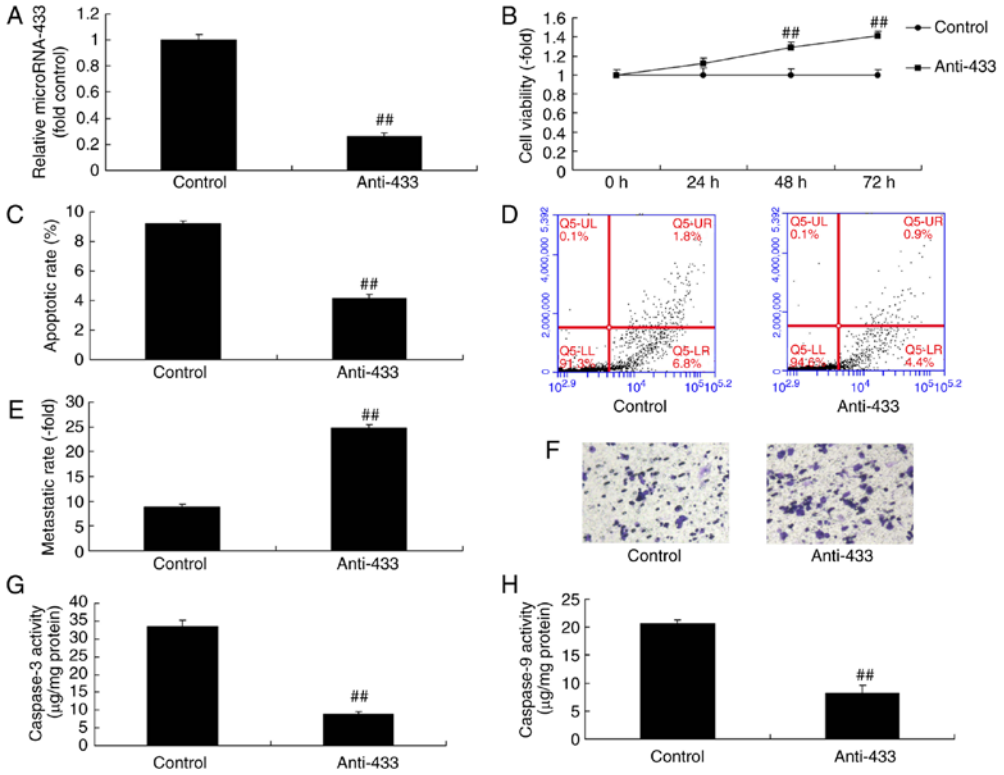

Figure 2. Downregulation of microRNA-433 promotes cell growth and inhibits apoptosis of cervical cancer cells. (A) Expression of microRNA-433; (B) cell viability; (C) apoptotic rate; (D) flow cytometry of apoptosis; (E) metastatic rate (magnification, x200); (F) staining for apoptosis; (G) caspase-3 and (H) caspase-9 activity levels. Data are presented as the mean ± standard deviation. ##P<0.01, vs. control group. Control, negative control group; anti-433, downregulation of microRNA-433 group.

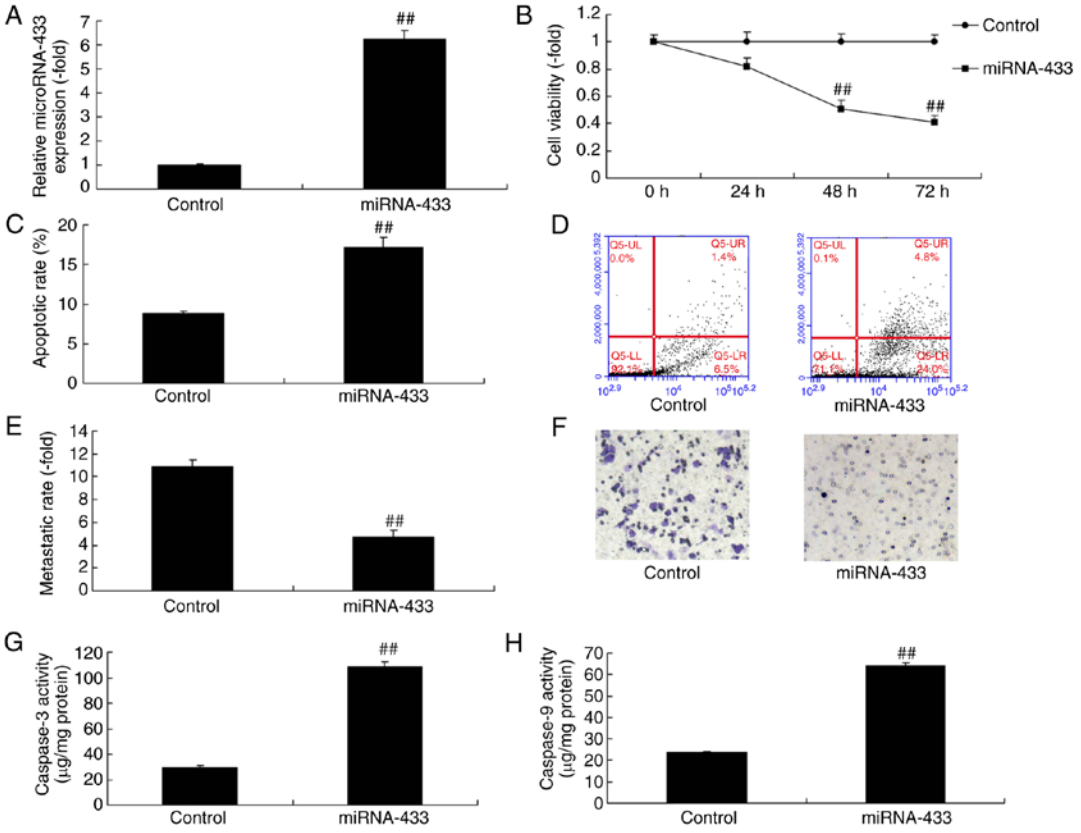

Figure 3. Upregulation of microRNA-433 reduces cell growth and promotes apoptosis of cervical cancer. (A) Expression of microRNA-433; (B) cell viability; (C) apoptotic rate; (D) flow cytometry of apoptosis (E) metastatic rate; (F) staining for metastasis (magnification, x200); (G) caspase-3 and (H) caspase-9 activity levels. Data are presented as the mean ± standard deviation. ##P<0.01 vs. control group. Control, negative control group; miRNA-433, upregulation of microRNA-433 group.

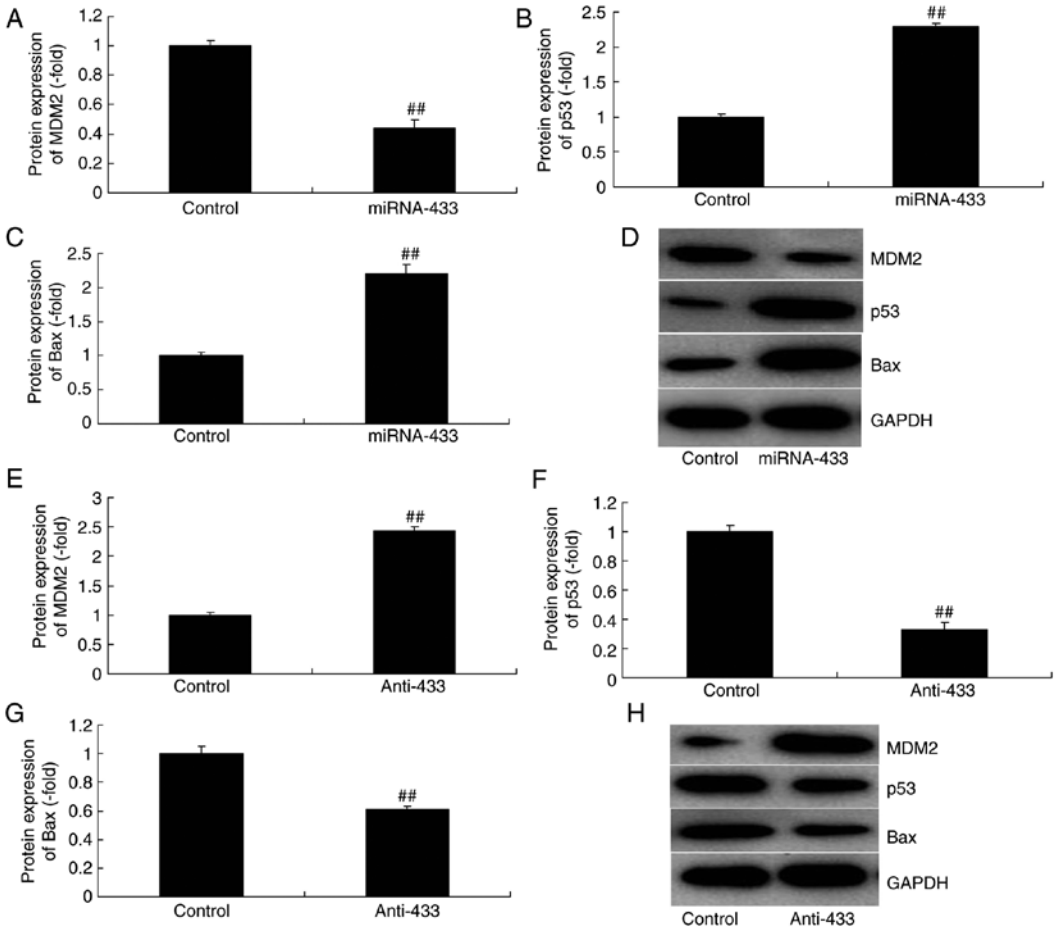

Figure 4. microRNA-433 regulates MDM2/p53/Bax signaling in cervical cancer. Statistical analysis of the protein expression of (A) MDM2, (B) p53 and (C) Bax in the miRNA-433 group from (D) western blot analysis. Statistical analysis of the protein expression of (E) MDM2, (F) p53 and (G) Bax in the anti-433 group from (H) western blot analysis. Data are presented as the mean ± standard deviation. $^{##}$P<0.01, vs. control group. Control, negative control group; miRNA-433, upregulation of microRNA-433 group; anti-433, downregulation of microRNA-433 group; Bax, B-cell lymphoma-2-associated X protein.

following transfection with microRNA-433 mimics, compared with that in the control group (Fig. 3A). The upregulation of microRNA-433 reduced the growth and metastasis, and promoted the apoptosis and caspase-3/-9 activity of the cervical cancer cells, compared with the control group (Fig. 3B-H).

MicroRNA-433 regulates MDM2/p53/Bax signaling in cervical cancer. It was also found that the overexpression of microRNA-433 induced the protein expression of p53 and Bax, and suppressed that of MDM2 in cervical cancer, compared with levels in the control group (Fig. 4A-D). However, the downregulation of microRNA-433 suppressed the protein expression of p53 and Bax, and induced that of MDM2 in cervical cancer, compared with levels in the control group (Fig. 4E-H).

MicroRNA-433 regulates FAK/PI3K/AKT signaling in cervical cancer. The present study attempted to confirm the mechanism of microRNA-433 in the growth and metastasis of cervical cancer cells. MicroRNA-433 was found to target FAK mRNA (Fig. 5A). The immunofluorescence staining showed that the downregulation of microRNA-433 induced the protein expression of FAK, PI3K and p-Akt in cervical cancer, compared with the their levels in the control group (Fig. 5B). The overexpression of microRNA-433 suppressed the protein expression of FAK, PI3K and p-Akt in cervical cancer, compared with their levels in the control group, whereas the downregulation of microRNA-433 induced the protein expression of FAK and p-Akt in cervical cancer, compared with their levels in the control group (Fig. 5C-F). These results indicated that FAK/PI3K/AKT signaling is important in the effect of microRNA-433 on cervical cancer cell growth.

Activation of FAK inhibits the effect of microRNA-433 on the growth of cervical cancer cells. To further confirm the role of FAK in the effect of microRNA-433 on the growth of cervical cancer cells, a FAK plasmid was used to induce the protein expression of FAK, PI3K and p-Akt in cervical cancer cells following microRNA-433 induction (Fig. 6A-D). The activation of FAK suppressed the protein expression of p53 and Bax, and induced that of MDM2 in cervical cancer cells following microRNA-433 induction, compared with the microRNA-433 group (Fig. 6E-H). The activation of FAK increased the growth and metastasis, and reduced the apoptotic rate of the cervical cancer cells, compared with cells in the microRNA-433 group (Fig. 7A-E). The microRNA-433-induced activities of caspase-3/-9 in cervical cancer cells were decreased by the activation of FAK, compared with levels in the microRNA-433 group (Fig. 7F and G).

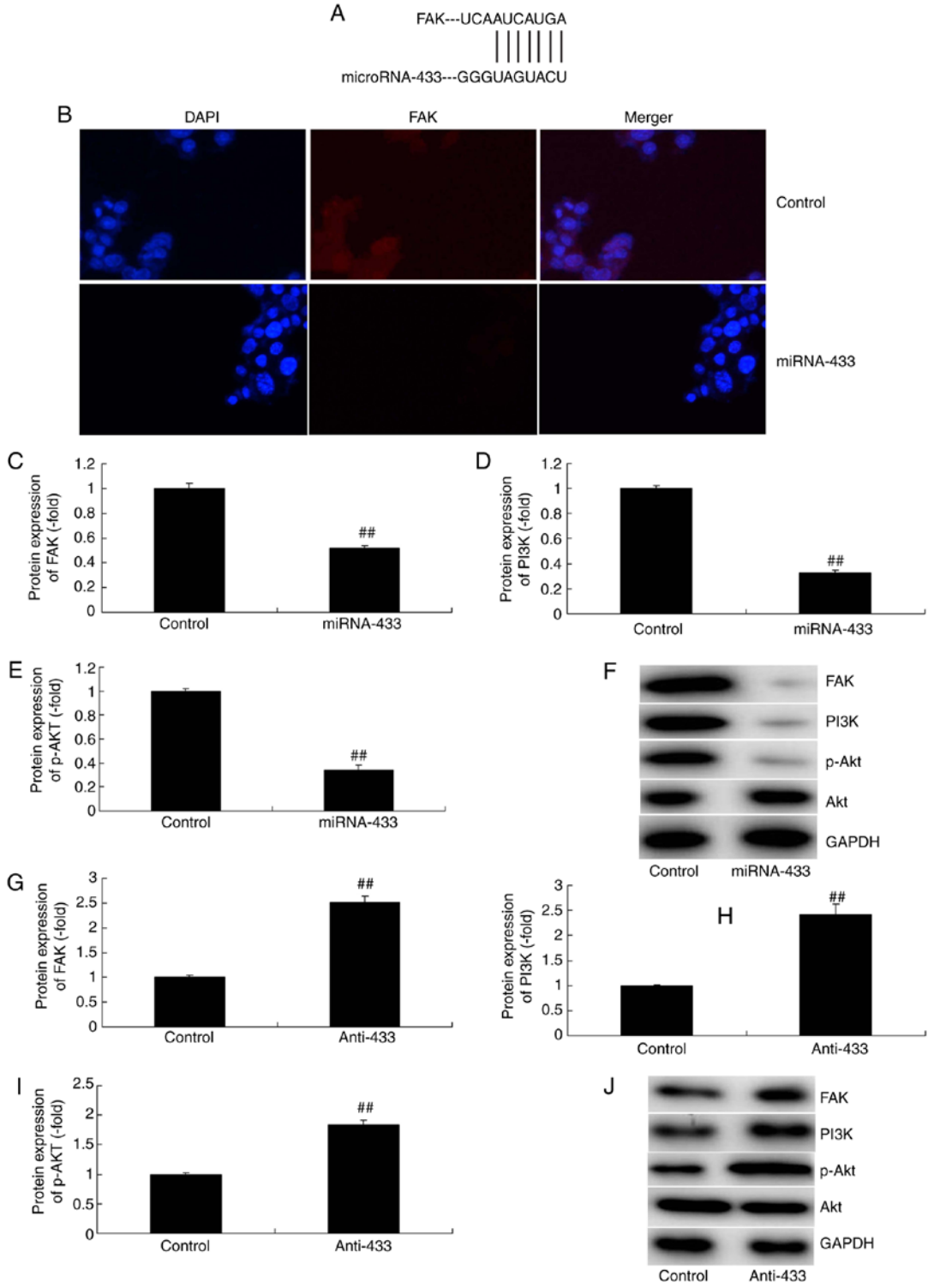

Figure 5. MicroRNA-433 regulates FAK/PI3K/AKT signaling in cervical cancer. (A) MicroRNA-433 targets FAK mRNA. (B) Immunofluorescence (magnification, x400) for FAK protein expression. Statistical analysis of the protein expression of (C) FAK, (D) PI3K and (E) p-AKT in the miRNA-433 group from (F) western blot analysis. Statistical analysis of the protein expression of (G) FAK, (H) PI3K and (I) p-AKT in the anti-433 group from (J) western blot analysis. Data are presented as the mean ± standard deviation. $^{\#\#}$P<0.01, vs. control group. Control, negative control group; miRNA-433, upregulation of microRNA-433 group; anti-433, downregulation of microRNA-433 group; FAK, focal adhesion kinase; PI3K, phosphoinositide 3-kinase; p-, phosphorylated.

Inhibition of AKT reduces the effect of microRNA-433 on the growth of cervical cancer cells. To further confirm the role of AKT in the effect of microRNA-433 on cervical cancer cell growth, 0.1 nM of GDC-0032 (MedChemExpress), an Akt inhibitor, was used. The Akt inhibitor reduced the protein expression PI3K, p-Akt and MDM2, and increased the expression of p53 and Bax in cervical cancer in the anti-microRNA-433 group, compared with expression levels in the anti-microRNA-433 group (Fig. 8A-G). In addition, the inhibition of AKT reduced the effect of microRNA-433 on the growth, metastasis and apoptotic rate of the cervical cancer cells, compared with the anti-microRNA-433

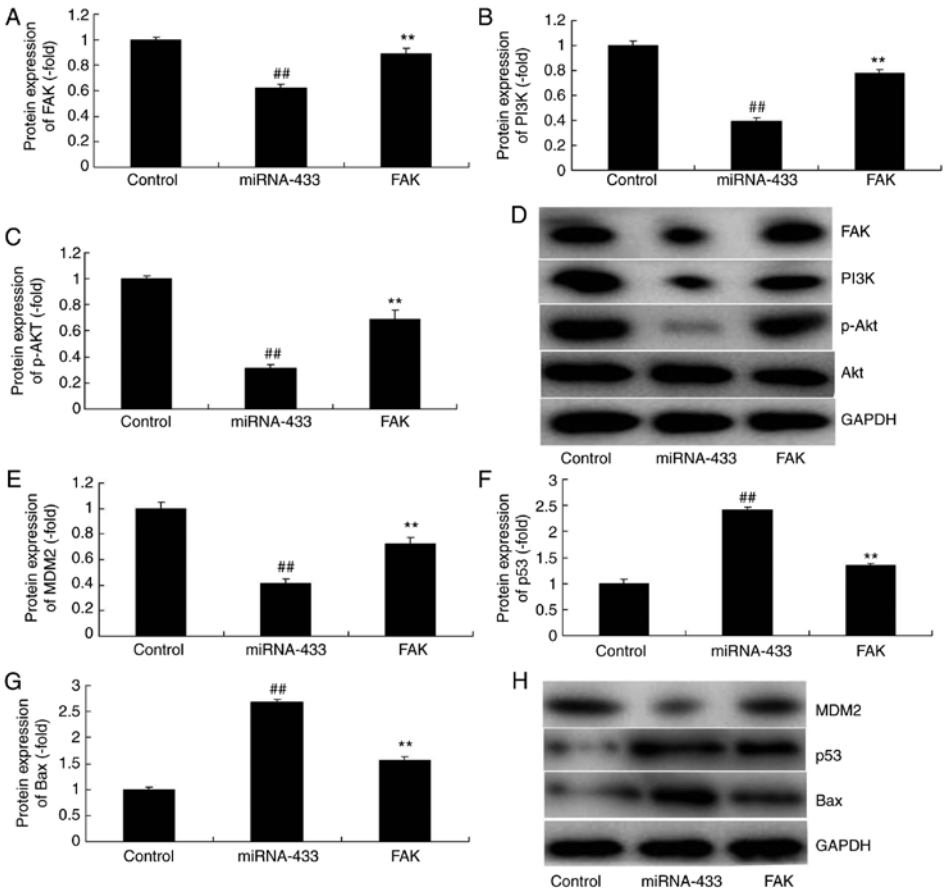

Figure 6. Activation of FAK affects the function of microRNA-433 on cell growth in cervical cancer. Statistical analysis of the protein expression of (A) FAK, (B) PI3K and (C) p-AKT from (D) western blot analysis. Statistical analysis of the protein expression of (E) MDM2, (F) p53 and (G) Bax from (H) western blot analysis. Data are presented as the mean ± standard deviation. ##P<0.01, vs. control group, **P<0.01 vs. miRNA-433 group. Control, negative control group; miRNA-433, upregulation of microRNA-433 group; FAK group, upregulation of microRNA-433 and FAK plasmid group; FAK, focal adhesion kinase; PI3K, phosphoinositide 3-kinase; p-, phosphorylated; Bax, B-cell lymphoma-2-associated X protein.

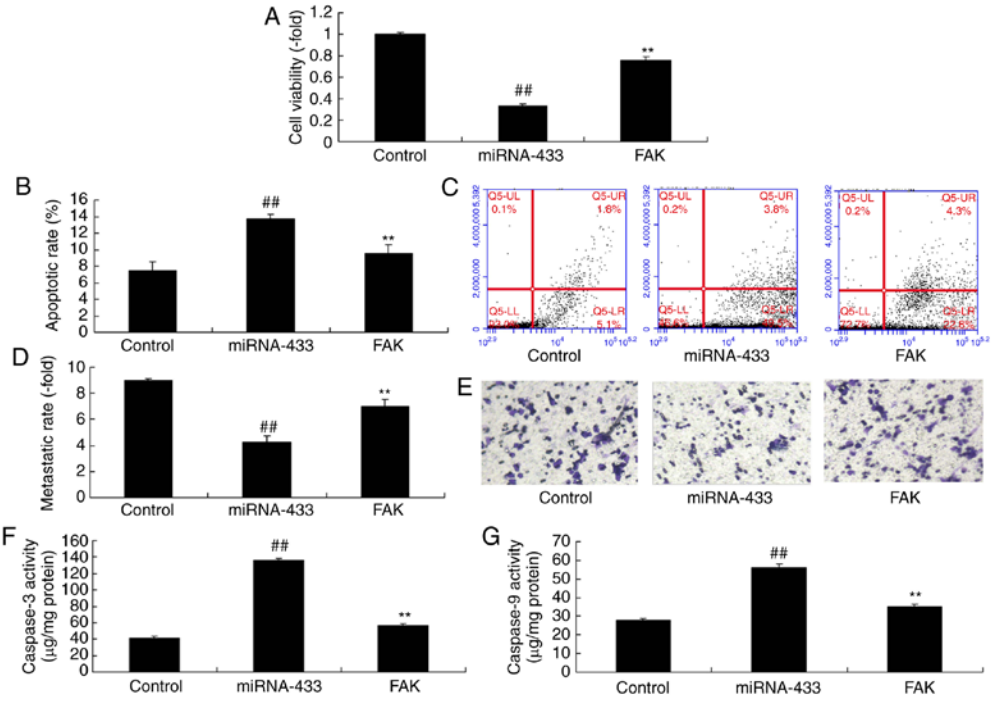

Figure 7. Activation of FAK affects the function of microRNA-433 on cell growth in cervical cancer. (A) Cell viability; (B) apoptotic rate; (C) flow cytometry of apoptosis; (D) metastatic rate; (E) staining for metastasis (magnification, x200); (F) caspase-3 and (G) caspase-9 activity levels. Data are presented as the mean ± standard deviation. ##P<0.01, vs. control group, **P<0.01, vs. miRNA-433 group. Control, negative control group; miRNA-433, upregulation of microRNA-433 group; FAK group, upregulation of microRNA-433 and FAK plasmid group. FAK, focal adhesion kinase.

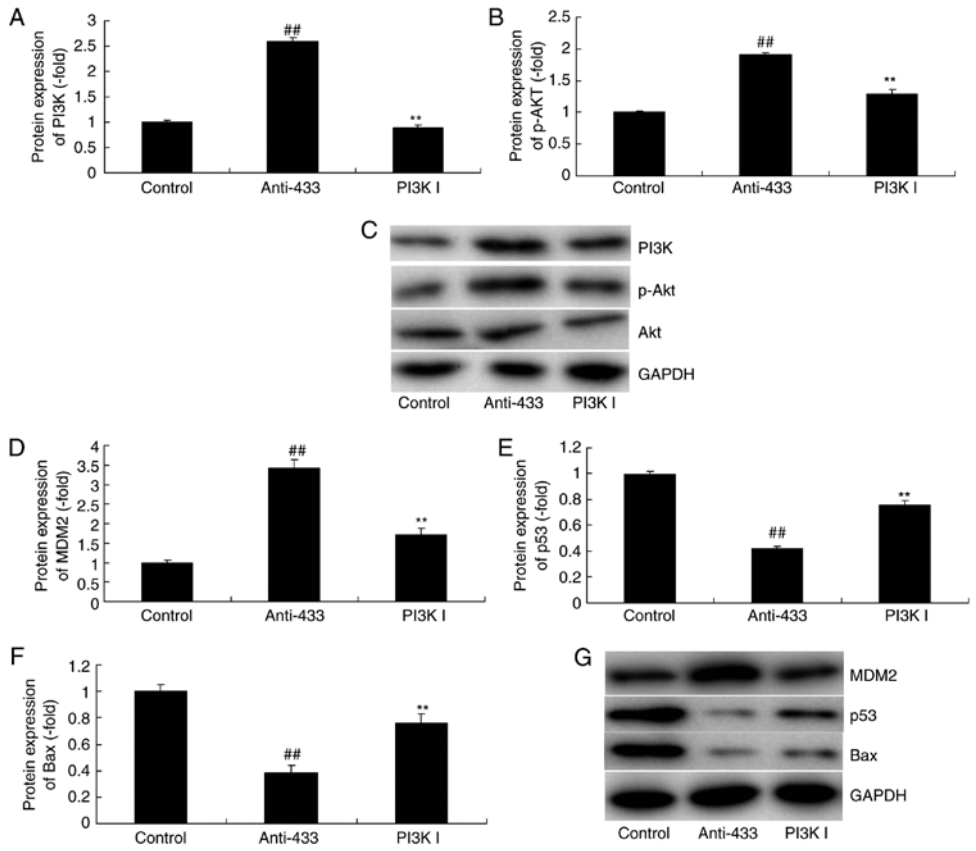

Figure 8. Inhibition of AKT reduces the function of microRNA-433 on cell growth in cervical cancer. Statistical analysis of the protein expression of (A) PI3K and (B) p-AKT from (C) western blot analysis, and of (D) MDM2, (E) p53 and (F) Bax from (G) western blot analysis. Data are presented as the mean ± standard deviation. $^{\#\#}$P<0.01, vs. control group, **P<0.01, vs. miRNA-433 group. Control, negative control group; anti-433, downregulation of microRNA-433 group; PI3K I, downregulation of microRNA-433 and AKT inhibitor group. PI3K, phosphoinositide 3-kinase p-, phosphorylated; Bax, B-cell lymphoma-2-associated X protein.

group (Fig. 9A-E). Additionally, the anti-microRNA-433-inhibited activities of caspase-3/-9 in the cervical cancer cells were increased by the AKT inhibitor, compared with levels in the anti-microRNA-433 group (Fig. 9F and G). These results indicated that AKT was important in the effect of microRNA-433 on cervical cancer cell growth.

Discussion

Cervical cancer is the most common malignancy in Chinese women and is also a major contributor to patient mortality rates (1). Cervical cancer is a malignancy deriving from the cervical squamo-columnar junction squamous epithelial cells and gland (1). It has three pathological types, namely, squamous carcinoma, adenocarcinoma and adenosquamous carcinoma. Of these, cervical squamous carcinoma accounts for ~80% of cases (13). Heteromorphism is observed in atypical hyperplasia of the cervical squamous epithelium in all layers of the squamous epithelium. In addition, it invades the mesenchyme and transfers to other sites to develop invasive carcinoma. This process forms a continuous lesion, which frequently occurs over 10 years (14). Early identification and timely treatment can substantially improve the survival rate of patients with cervical squamous carcinoma (15). Therefore, investigating the mechanisms underlying the invasion and metastasis of cervical cancer cell is of the highest priority (16). In the present study, the downregulated expression of microRNA-433 in patients with cervical cancer was investigated. Liang *et al* showed that microRNA-433 inhibits the migration and invasion of ovarian cancer cells via targeting Notch1 (17). In the present study, only one cell line was used, which is a limitation of the study. Additional cell lines or an animal model are to be used in further investigations.

MicroRNAs can promote cell proliferation, cell cycle rearrangement and cell differentiation. In addition, they can regulate transcription through RNA polymerase (18). Therefore, microRNAs can accelerate cell differentiation and proliferation, and promote cancerous development (5). They can also regulate the immune system, cell apoptosis, anti-apoptosis and inflammatory responses (13). Therefore, they can regulate disease genesis and development (18). In the present study, it was found that the DFS and OS rates of patients with low microRNA-433 were lower, compared with those of patients with high microRNA-433. Yang *et al* revealed that microRNA-433 inhibits liver cancer cell migration (19).

FAK is a novel tyrosine protein kinase identified by Schaller *et al* in 1992 and is the central molecule of the integrin-mediated signal transduction pathway (20). It is closely associated with cell adhesion, proliferation, migration, and apoptosis. Furthermore, it is involved in tumor invasion and metastasis (21). Evidence indicates that the expression of FAK is upregulated in invasive cells, including those in ovarian cancer,

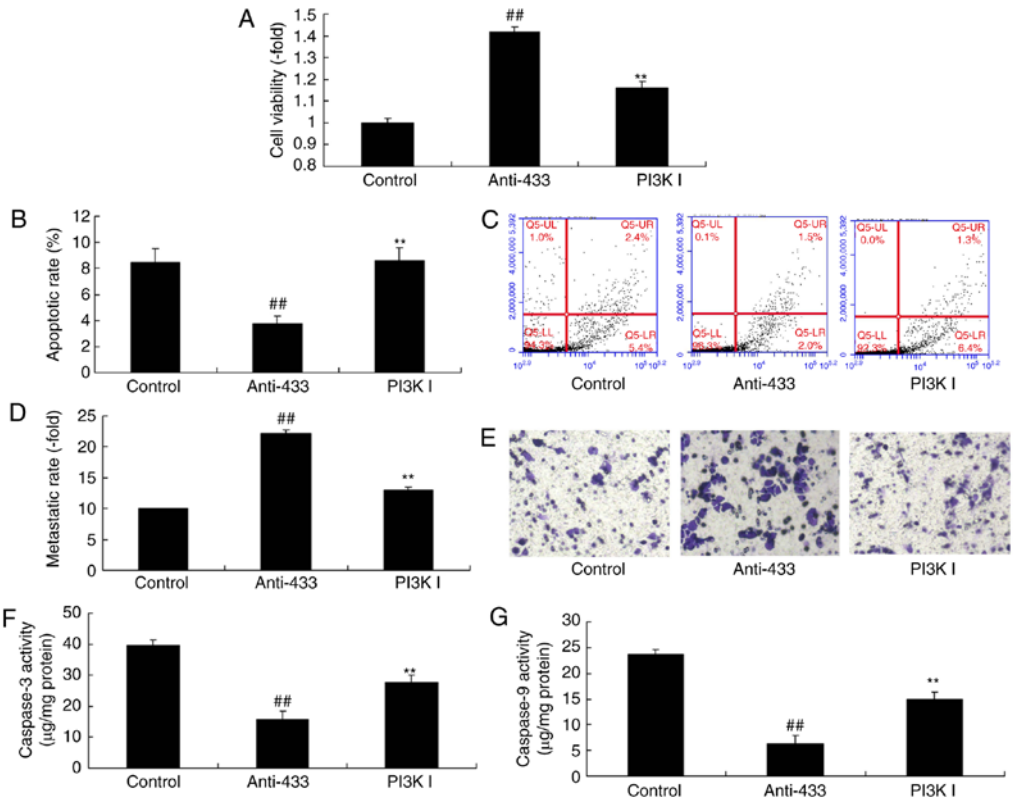

Figure 9. Inhibition of AKT reduces the function of microRNA-433 on cell growth in cervical cancer. (A) Cell viability, (B) apoptotic rate; (C) flow cytometry of apoptosis, (D) metastatic rate and (E) staining for metastasis (magnification, x200); (F) caspase-3 and (G) caspase-9 activity levels. Data are presented as the mean ± standard deviation. ##P<0.01, vs. control group, **P<0.01, vs. anti-433 group. Control, negative control group; anti-433, downregulation of microRNA-433 group; PI3K I, downregulation of microRNA-433 and AKT inhibitor group. PI3K, phosphoinositide 3-kinase.

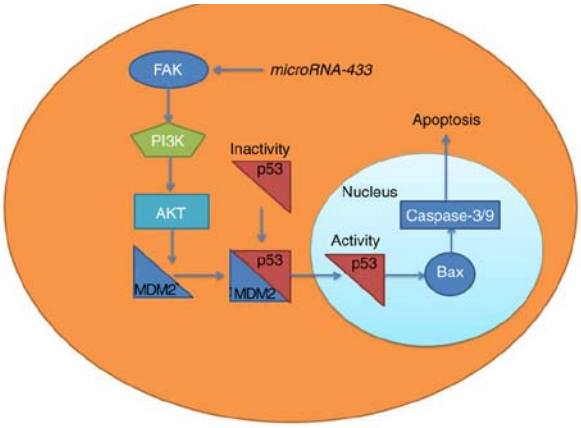

Figure 10. MicroRNA-433 inhibits cell growth and induces apoptosis in human cervical cancer through PI3K/AKT signaling by targeting FAK. FAK, focal adhesion kinase; PI3K, phosphoinositide 3-kinase; Bax, B-cell lymphoma 2-associated X protein.

endometrial cancer and thyroid carcinoma (8). It has been found that the overexpression of FAK represents an early stage during the genesis of head and neck cancer, and the activation of FAK may promote lymph node metastasis (21). Therefore, the overexpression of FAK may be a common pathway for the invasion and metastasis potentials of all tumor types. In addition, the expression level of FAK may serve as an early marker of tumor invasion and metastasis (20). The results of the present study suggested that the overexpression of microRNA-433 suppressed the protein expression of FAK, PI3K and p-Akt in cervical cancer. Wang *et al* reported that microRNA-433 downregulates FAK to inhibit the proliferation, migration, and invasiveness of SCC-9 oral squamous cell carcinoma cells (22).

Akt, also known as protein kinase B, is a serine/threonine kinase. The phosphorylation of its active regions, Thr308 and C-terminal Ser473, is required for its complete activation (23). The activation of Akt can regulate multiple downstream target proteins, including the forkhead box O family, nuclear factor-κB and mTOR (24). In addition, it can regulate cell proliferation and survival by activating or inhibiting these downstream signaling molecules through phosphorylation (23,24). Following activation, Akt can promote the glycolytic pathway in tumor cells; it can also regulate Bcl-2 family protein activity through glucose metabolism activity (25). Therefore, it can inhibit cell apoptosis. The results of the present study showed that the inhibition of PI3K inhibited the function of anti-microRNA-433 on the growth of cervical cancer cells. Xue *et al* reported that microRNA-433 inhibits cell proliferation in hepatocellular carcinoma via PI3K/AKT signaling (26). In the present study, an AKT inhibitor (GDC-0032) was used, and drug activators or inhibitors are to be examined in further investigations.

It has been suggested that the expression of microRNA-433 is downregulated in patients with cervical cancer. MicroRNA-433 suppressed cancer cell growth in cervical cancer via FAK/PI3K/AKT signaling (Fig. 10), thereby providing a novel option for the treatment of cervical cancer. This link between microRNA-433 and FAK/PI3K/AKT

signaling identifies a novel potential therapeutic target for the treatment of cervical cancer.

Acknowledgements

Not applicable.

Funding

No funding was received.

Availability of data and materials

The analyzed data sets generated during the study are available from the corresponding author on reasonable request.

Authors' contributions

WZ designed the experiment; JX, LC and LL performed the experiment; WZ and JX analyzed the data; WZ wrote the manuscript. All authors read and approved the final manuscript.

Ethics approval and consent to participate

This study was approved by the Ethics Committee of The Second Affiliated Hospital of Suzhou University. Informed patient consent was obtained prior to participation.

Patient consent for publication

Not applicable.

Competing interests

The authors declare that they have no competing interests.

References

1. Gemma M, Scola E, Baldoli C, Mucchetti M, Pontesilli S, De Vitis A, Falini A and Beretta L: Auditory functional magnetic resonance in awake (nonsedated) and propofol-sedated children. Paediatr Anaesth 26: 521-530, 2016.
2. Zheng Y, Bu J, Yu L, Chen J and Liu H: Nobiletin improves propofol-induced neuroprotection via regulating Akt/mTOR and TLR 4/NF-κB signaling in ischemic brain injury in rats. Biomed Pharmacother 91: 494-503, 2017.
3. Liu Y, Gong Y, Wang C, Wang X, Zhou Q, Wang D, Guo L, Pi X, Zhang X, Luo S, *et al*: Online breath analysis of propofol during anesthesia: Clinical application of membrane inlet-ion mobility spectrometry. Acta Anaesthesiol Scand 59: 319-328, 2015.
4. Hua FZ, Ying J, Zhang J, Wang XF, Hu YH, Liang YP, Liu Q and Xu GH: Naringenin pre-treatment inhibits neuroapoptosis and ameliorates cognitive impairment in rats exposed to isoflurane anesthesia by regulating the PI3/Akt/PTEN signalling pathway and suppressing NF-κB-mediated inflammation. Int J Mol Med 38: 1271-1280, 2016.
5. Chen X, Du YM, Xu F, Liu D and Wang YL: Propofol prevents hippocampal neuronal loss and memory impairment in cerebral ischemia injury through promoting PTEN degradation. J Mol Neurosci 60: 63-70, 2016.
6. Chen X, Wang W, Zhang J, Li S, Zhao Y, Tan L and Luo A: Involvement of caspase-3/PTEN signaling pathway in isoflurane-induced decrease of self-renewal capacity of hippocampal neural precursor cells. Brain Res 1625: 275-286, 2015.
7. Wang LY, Tang ZJ and Han YZ: Neuroprotective effects of caffeic acid phenethyl ester against sevoflurane induced neuronal degeneration in the hippocampus of neonatal rats involve MAPK and PI3K/Akt signaling pathways. Mol Med Rep 14: 3403-3412, 2016.
8. Ma J, Xiao W, Wang J, Wu J, Ren J, Hou J, Gu J, Fan K and Yu B: Propofol inhibits NLRP3 inflammasome and attenuates blast-induced traumatic brain injury in rats. Inflammation 39: 2094-2103, 2016.
9. Xiao R, Gan M and Jiang T: Wogonoside exerts growth-suppressive effects against T acute lymphoblastic leukemia through the STAT3 pathway. Hum Exp Toxicol 36: 1169-1176, 2017.
10. Karnati HK, Panigrahi MK, Gutti RK, Greig NH and Tamargo IA: miRNAs: Key players in neurodegenerative disorders and epilepsy. J Alzheimers Dis 48: 563-580, 2015.
11. Liu EY, Cali CP and Lee EB: RNA metabolism in neurodegenerative disease. Dis Model Mech 10: 509-518, 2017.
12. Livak KJ and Schmittgen TD: Analysis of relative gene expression data using real-time quantitative PCR and the $2^{-\Delta\Delta CT}$ method. Methods 25: 402-408, 2001.
13. Wang Y, Wu C, Han B, Xu F, Mao M, Guo X and Wang J: Dexmedetomidine attenuates repeated propofol exposure-induced hippocampal apoptosis, PI3K/Akt/Gsk-3β signaling disruption, and juvenile cognitive deficits in neonatal rats. Mol Med Rep 14: 769-775, 2016.
14. Chen B, Deng X, Wang B and Liu H: Persistent neuronal apoptosis and synaptic loss induced by multiple but not single exposure of propofol contribute to long-term cognitive dysfunction in neonatal rats. J Toxicol Sci 41: 627-636, 2016.
15. Kim JH, Kim BK, Kim DW, Shin HY, Yu SB, Kim DS, Ryu SJ, Kim KH, Jang HK and Kim JD: Effect of propofol on microRNA expression profile in adipocyte-derived adult stem cells. Chonnam Med J 50: 86-90, 2014.
16. Eberl S, Preckel B, Bergman JJ, van Dieren S and Hollmann MW: Satisfaction and safety using dexmedetomidine or propofol sedation during endoscopic oesophageal procedures: A randomised controlled trial. Eur J Anaesthesiol 33: 631-637, 2016.
17. Liang T, Guo Q, Li L, Cheng Y, Ren C and Zhang G: MicroRNA-433 inhibits migration and invasion of ovarian cancer cells via targeting Notch1. Neoplasma 63: 696-704, 2016.
18. Zhang J, Xia Y, Xu Z and Deng X: Propofol suppressed hypoxia/reoxygenation-induced apoptosis in HBVSMC by regulation of the expression of Bcl-2, bax, caspase3, kir6.1, and p-JNK. Oxid Med Cell Longev 2016: 1518738, 2016.
19. Yang Z, Tsuchiya H, Zhang Y, Hartnett ME and Wang L: MicroRNA-433 inhibits liver cancer cell migration by repressing the protein expression and function of cAMP response element-binding protein. J Biol Chem 288: 28893-28899, 2013.
20. An K, Shu H, Huang W, Huang X, Xu M, Yang L, Xu K and Wang C: Effects of propofol on pulmonary inflammatory response and dysfunction induced by cardiopulmonary bypass. Anaesthesia 63: 1187-1192, 2008.
21. Zhou CH, Zhu YZ, Zhao PP, Xu CM, Zhang MX, Huang H, Li J, Liu L and Wu YQ: Propofol inhibits lipopolysaccharide-induced inflammatory responses in spinal astrocytes via the toll-like receptor 4/MyD88-dependent nuclear factor-κB, extracellular signal-regulated protein kinases1/2, and p38 mitogen-activated protein kinase pathways. Anesth Analg 120: 1361-1368, 2015.
22. Wang YJ, Zhang ZF, Fan SH, Zhuang J, Shan Q, Han XR, Wen X, Li MQ, Hu B, Sun CH, *et al*: MicroRNA-433 inhibits oral squamous cell carcinoma cells by targeting FAK. Oncotarget 8: 100227-100241, 2017.
23. Li M, Yang HM, Luo DX, Chen JZ and Shi HJ: Multi-dimensional analysis on parkinson's disease questionnaire-39 in parkinson's patients treated with bushen huoxue granule: A multicenter, randomized, double-blinded and placebo controlled trial. Complement Ther Med 29: 116-120, 2016.
24. Leavy B, Kwak L, Hagstromer M and Franzen E: Evaluation and implementation of highly challenging balance training in clinical practice for people with Parkinson's disease: Protocol for the hibalance effectiveness-implementation trial. BMC Neurol 17: 27, 2017.
25. van de Weijer SC, Duits AA, Bloem BR, Kessels RP, Jansen JF, Köhler S, Tissingh G and Kuijf ML: The Parkin'Play study: Protocol of a phase II randomized controlled trial to assess the effects of a health game on cognition in Parkinson's disease. BMC Neurol 16: 209, 2016.
26. Xue J, Chen LZ, Li ZZ, Hu YY, Yan SP and Liu LY: MicroRNA-433 inhibits cell proliferation in hepatocellular carcinoma by targeting p21 activated kinase (PAK4). Mol Cell Biochem 399: 77-86, 2015.